HHS Public Access

Author manuscript

Dev Biol. Author manuscript; available in PMC 2020 September 15.

Published in final edited form as:

Dev Biol. 2019 September 15; 453(2): 168–179. doi:10.1016/j.ydbio.2019.05.015.

Ubiquitination is required for the initial removal of paternal organelles in *C. elegans*

Paola Molina,

Department of Biology, Middle Tennessee State University, 1301 E. Main St, Murfreesboro, TN 37132, USA

Yunki Lim,

School of Medicine and Dentistry, University of Rochester Medical Center, Rochester, NY, 14642, USA

Lynn Boyd

Department of Biology, Middle Tennessee State University, 1301 E. Main St, Murfreesboro, TN 37132, USA

Abstract

Elimination of paternal mitochondria after fertilization occurs in many species using the process of selective autophagy. The mechanism for targeting paternal mitochondria, but not maternal mitochondria, for elimination in the early embryo is not well understood. The results in this paper suggest that there are at least two different mechanisms for targeting paternal mitochondria for elimination: the first involving ubiquitination and a second involving a mitochondrial associated autophagy receptor, *fndc-1.* Elimination of paternal mitochondria can be visualized in embryos of the nematode, *C. elegans.* Paternal mitochondria enter the zygote at fertilization. Initially, they are closely associated with another sperm organelle, the membraneous organelle (MO). The MOs become ubiquitinated within minutes after fertilization. Simultaneous RNAi knockdown of two ubiquitin conjugating enzymes, *ubc-18* and *ubc-16*, reduces MO ubiquitination. Loss of function of *ubc-18* alone leads to loss of K48-linked polyubiquitin chains and halts the recruitment of proteasome to MOs. Interestingly, knockdown of *ubc-18* or *ubc-16* or the combination does not reduce the localization of K63-linked ubiquitin chains to MOs suggesting that some ubiquitin structure other than K63 chains is responsible for recruiting the autophagy machinery to MOs. Double knockdown (*ubc-18/ubc-16*) inhibits the recruitment of the autophagy protein, LGG-1 (homolog of LC3/GABARAP), to paternal organelles and causes the persistence of paternal mitochondria into the two cell stage. If paternal mitochondria are not eliminated via this early process, they are eventually removed from the embryo in a process that depends on the mitophagy adaptor protein, *fndc-1.* Thus, there are two redundant, but temporally distinct mechanisms that target paternal mitochondria for elimination in *C. elegans*. In addition to the involvement of ubiquitination in the elimination of paternal mitochondria, two subunits of the proteasome, *rpn-10*

Corresponding Author: Lynn Boyd lynn.boyd@mtsu.edu.

and *rad-23*, are required for elimination of paternal mitochondria. These subunits are known to function as ubiquitin receptors and knockdown of either inhibits the recruitment of proteasome to ubiquitinated MOs. Their knockdown does not affect the localization of LGG-1 to paternal structures indicating that the proteasome is not required for autophagy membrane recruitment but might be involved in autophagosome maturation or its fusion with the lysosome.

Keywords

ubiquitin; proteasome; mitophagy; paternal mitochondria elimination; ubiquitin conjugating enzyme (UBC)

Introduction:

Elimination of organelles from the cell involves the process of autophagy. Selective autophagy is a mechanism where specific cell structures are targeted for autophagy (Gatica et al., 2018). Selective autophagy has been implicated in the removal of paternal mitochondria after fertilization (Sato and Sato, 2017). The current study examines the pathway for targeting paternal organelles for selective autophagy.

Most animals inherit the mitochondrial genome of their mother and not their father (Hutchison et al., 1974). The mechanism for uniparental inheritance of mitochondria is not obvious since fertilization is the result of the fusion of two cells, the oocyte and the sperm, both of which contain their own mitochondria. A flurry of papers in the past decade have explored possible mechanisms of paternal mitochondria elimination and have suggested the involvement of a variety of pathways including mitochondrial DNA degradation, fission-fusion disruption, and ubiquitination (Sato and Sato, 2017). The presumed ultimate fate of the paternal mitochondrion is degradation in the lysosome via the autophagy pathway. Indeed, disruption of the autophagy pathway inhibits paternal mitochondria elimination (Al Rawi et al., 2011; Sato and Sato, 2011). A persistent question has been what is responsible for selectively degrading paternal mitochondria versus the more abundant maternal mitochondria.

Selective autophagy depends on the interactions between cargo and the LC3/GABARAP autophagy proteins (Gatica et al., 2018). Cargo adaptor proteins that contain LIR (LC3 interacting) domains are used to recruit the autophagosome machinery. Ubiquitination can serve as a cargo recognition signal for autophagy. K63-linked chains are recognized by p62 or other cargo adaptor proteins that bind to polyubiquitin (Gatica et al., 2018; Geisler et al., 2010; Huynh et al., 2007; Matsumoto et al., 2011). Other autophagy adapter proteins have also been identified including BNIP3, NIX, and FUNDC1 (Yoo and Jung, 2018).

In *Drosophila*, mammals, and *C. elegans*, autophagy and the ubiquitin-proteasome system are essential for the removal of paternal mitochondria (Al Rawi et al., 2011; Politi et al., 2014; Sato and Sato, 2011; Sato et al., 2018). In mammals, sperm mitochondria are ubiquitinated before they enter the oocyte (Hutchison et al., 1974; Sutovsky et al., 1999, 2000). Experiments in porcine embryos suggest that proteasome activity is also required for the elimination of paternal mitochondria in mammals (Sutovsky et al., 2003). While

Drosophila also utilizes ubiquitin (Ub) and autophagy components, their process of elimination appears to be different (Chan and Schon, 2012; DeLuca and O'Farrell, 2012; Politi et al., 2014). In *Drosophila*, after fertilization paternal mitochondria are tagged with K63 chains and autophagy proteins similar to what has been seen with paternal organelles in *C. elegans* (Politi et al., 2014). However, in *Drosophila* paternal mitochondrial DNA degradation by mitochondrial endonuclease G begins before fertilization (DeLuca and O'Farrell, 2012) rather than after fertilization as in *C. elegans* (Zhou et al., 2016).

Studies in *C. elegans* have examined the removal of two types of paternal organelles, the paternal mitochondria and the membranous organelles (MOs) (Al Rawi et al., 2011; Djeddi et al., 2015; Sato and Sato, 2011; Sato et al., 2018). MOs are nematode specific Golgi derived vesicles (Roberts et al., 1986). Prior to sperm activation, the MOs are associated with major sperm proteins (MSP). However, upon activation, the MSPs become localized to the pseudopod and the MOs remain in the cell body with many MOs fusing with the sperm plasma membrane. The full function of these organelles remains unknown. It has been proposed that removal of the MOs and paternal mitochondria might be linked, but this hypothesis has not been fully tested. MOs become ubiquitinated with K48 and K63 polyubiquitin chains soon after fertilization (Al Rawi et al., 2011). The ubiquitinated MOs and paternal mitochondria cluster together and are surrounded by autophagosome membranes during meiosis II (Djeddi et al., 2015; Hajjar et al., 2014). MOs along with paternal mitochondria are removed via autophagosome formation, the lysosome, and the autophagy receptor ALLO-1 (Al Rawi et al., 2011; Sato et al., 2018; Zhou et al., 2011). Recently it was shown that the complete block of ubiquitination prevented the recruitment of autophagy markers to MOs (Sato et al., 2018), but specific inhibition of the ubiquitination on paternal organelles has not been achieved.

Ubiquitination of substrates is guided by three enzymes: E1, E2 and E3. The E1, ubiquitin activating enzyme is responsible for an ATP dependent reaction where Ub+AMP remains bound to the E1 until a thioester bond is formed with the cysteine on the E1 (Soss et al., 2013). Then, ubiquitin is transferred to a cysteine at the active site of the E2 enzyme. The E2 ubiquitin conjugating enzyme (UBC) catalyzes the transfer of Ub to a lysine on the targeted substrate forming an isopeptide bond. Alternatively, the UBC can transfer Ub to a catalytic cysteine found on a HECT or RBR E3, which then transfers ubiquitin onto the targeted substrate forming an isopeptide bond (Vittal et al., 2013). Ubiquitination can occur as the addition of a single ubiquitin, monoubiquitination, or the formation of a ubiquitin chain, polyubiquitination, utilizing one of seven lysines on the ubiquitin protein. The interactions between the UBC and E3 and substrate designate the type of Ub modification (Christensen et al., 2007; Rodrigo-Brenni et al., 2010). Ubiquitin modifications such as K48 and K63 linked chains are used as signals for adaptor proteins. During autophagy, K63 chains are recognized by autophagy adaptor proteins such as p62 which then recruit the autophagosome membranes (Bjorkoy et al., 2005). K48 chains on proteins are commonly recognized by the proteasome and result in protein degradation (Chan et al., 2011; Husnjak et al., 2008; Rodrigo-Brenni et al., 2010). Therefore, to better understand the role of ubiquitin in the selection of paternal mitochondria for degradation it is important to identify the specific enzymes responsible for tagging the paternal organelles.

The current study investigates the role of post fertilization ubiquitination of MOs in *C. elegans* and how it modulates downstream events leading to the removal of paternal mitochondria. After conducting an RNAi screen of the 24 *C. elegans* UBCs, our results showed that more than one UBC was responsible for ubiquitinating MOs. A double UBC knockdown screen revealed that the combination of *ubc-18* and *ubc-16* was required for ubiquitination of MOs. *ubc-18* is required for the addition of K48 chains on MOs and proteasome localization to these organelles during meiosis I. Our results suggest the presence of a ubiquitin dependent pathway that results in the degradation of MOs and early removal of paternal mitochondria. We also show that paternal mitochondria can be removed by a second, ubiquitin-independent pathway that functions after the first mitosis.

Materials and Methods:

Worm strains and maintenance

C. elegans strains were grow on nematode growth medium (NGM) seeded with a bacterial lawn of OP50 *E. coli* and incubated at 20° C or 25° C (Brenner, 1974). Wildtype, *ubc-18(ku354)*, and *fndc-1(ry14)* nematodes were grown at 20° C. Transgenic nematodes were grown at 25° C, except VIG19 which was grown at 16° C. Strains used in this study are listed in Table 1.

KWN775 *fndc-1(ry14) II; him-5(e1490) V* was a gift from Dr. Keith Nehrke, University of Rochester Medical Center. VIG19 *mex-5p::GFP::lgg-1 II* was a gift from Dr. Vincent Galy, Insitute de Biologie Paris Siene, Université Pierre et Marie Curie.

Male populations and mating

Male N2 populations were generated by soaking 20 L4 hermaphrodites in 7% ethanol in M9 buffer at 20° C for 20 minutes. F2 generations were screened for males. Males were maintained by mating 10-20 males with 1-2 hermaphrodites on 60 mm mating plates (NGM plates seeded with 100 μL saturated overnight OP50 *E. coli* culture). Matings between strains were performed by placing 10 hermaphrodites and 20-30 males on mating plates at 20° C overnight for N2 hermaphrodites and 25° C for transgenic hermaphrodites.

Antibodies

Primary antibodies used in this study at 1:100 concentrations were rabbit anti-K48 ubiquitin (Apu2 from Millipore), rabbit anti-K63 (Apu3 from Millipore) and mouse monoclonal 1CB4 which recognizes MOs (gift from Steve L'Hernault at Emory University). Secondary antibodies used for immunofluorescence at 1:100 concentration were goat anti-mouse FITC and goat anti-rabbit TRITC (Jackson ImmunoResearch Laboratories).

Antibody staining

Presence of K48 and K63 chains were determined using K48 and K63 specific antibodies. Co-localization of each chain with MOs was determined using chain antibodies co-stained with 1CB4 antibodies. Embryos were extracted from one day adults by cutting them open on poly-L-lysine-coated slides. Slides were placed in liquid nitrogen for 5 minutes and then fixed with methanol at −20° C for 20 minutes. Slides were incubated in primary antibody

overnight at 4° C and then incubated with secondary for 2 hours at room temperature. Primary and Secondary antibodies were diluted in PBST:30% NGS (normal goat serum) and washes were done in PBST (PBS with 0.5% Tween-20). Vectasheild (Vector Labs, Burlingame, CA) plus DAPI was used as the mounting medium. Slides were observed using the LSM 700 confocal microscope equipped with Zen Black software.

Mitotracker staining

N2 males were labeled with Mitotracker Red CMXRos (Invitrogen) as described in Hajjar et al (2014). 10-15 L4 hermaphrodites were added to mating plates containing 20 Mitotracker soaked N2 or *fndc-1(my14)* males. They were allowed to mate for 24 hours at 25° C. Embryos were observed 42- 48 hours after mating using Zeiss LSM 700 confocal microscope as previously described (Boyd et al., 2011).

Fluorescent microscopy

All fluorescent images were acquired using the Zeiss LSM 700 confocal microscope and analyzed using Zen Black software. For live cell and antibody staining experiments, the 488 nm laser was used for GFP and FITC, and 555 nm laser was used for mCherry, TRITC and Mitotracker red. DAPI imaging was performed using a 405 nm laser. Image settings were kept constant for each experiment.

RNAi by Feeding

RNAi knockdowns were achieved by feeding the worms bacteria expressing dsRNA for each gene of interest. RNAi clones were obtained from the Ahringer library or the Vidal ORF library (*ubc-18*)(Kamath et al., 2003; Rual et al., 2004). Simultaneous knockdowns were achieved by feeding worms a 1:1 mixture of each RNAi clone. All RNAi plasmids were in the HT115 strain background. Controls for the RNAi experiments included a L4440 plasmid (vector), as well as the embryonic lethal gene (*ubc-2*) as a positive control. The positive control was also diluted 1:1 with the empty vector to establish the efficiency of a double knockdown. RNAi clones were streaked from glycerol stocks onto tryptic soy agar with ampicillin (100μg/mL) and tetracycline (10 μg/mL) overnight. Then single colonies were inoculated in tryptic soy broth with ampicillin and tetracycline. Bacterial overnights were grown at 37° C in shaking incubator for 16 hours. NGM plates containing 0.2% lactose were seeded with bacterial overnights. L4 larvae were transferred to dry RNAi plates and allowed to grow at the appropriate temperature for each strain and observed after 24 hours. In experiments with double UBC knockdowns, worms were synchronized by bleaching method and then placed on RNAi plates as L1 larvae (Stiernagle, 2006). Worms were allowed to grow and their F1 generation L4 larvae were moved to fresh RNAi plates and examined after 24 hours.

Embryonic lethality assays

The assays were performed at 20° C. After respective RNAi treatments, F1 generation L4 larvae were placed on fresh RNAi plates for 24 hour and then removed. The total number of embryos were then scored. Hatching of embryos was scored after 24 hours. Embryonic

lethality percentages were calculated as the total number of hatched progeny over the total number of embryos.

Statistical Analysis

Each figure legends explains sample size for each experiment. Two sample *z*-tests were performed using VasarStats on data from Figure 1C. Fisher's exact test was performed on data that was less than 20 (Figure 3B and 4B) and to find significance in embryonic lethality study (supplemental Figure 2). Error bars presented in figures 1C, 3B, 4B, and 4D represent a 95% confidence interval and were derived using the modified Wald method on GraphPad. Student *t-test* was used to determine the significance of difference between groups and error bars representing SEM (Standard Error of the Mean) in figures 2A, 4D and 5B.

Results:

ubc-16 *and* ubc-18 *are required for clearance of membranous organelles*

During the process of fertilization in *C. elegans*, two organelles from the sperm are incorporated into the zygote: the sperm mitochondria and the membraneous organelles (MOs). The MOs, but not the mitochondria, become ubiquitinated in the zygote. The addition of ubiquitin to MOs occurs within minutes after fertilization (Al Rawi et al., 2011; Hajjar et al., 2014). In order to elucidate the pathway involved in this ubiquitination, an RNAi screen of ubiquitin conjugating enzymes (UBCs) was undertaken. All 24 ubiquitin conjugating enzymes were screened individually as well as all pairwise combinations (276 pairwise combinations). A transgenic worm with a GFP-tagged ubiquitin (GFP::Ub) that is expressed in the germline was used to visualize ubiquitinated MOs in the embryo (Figure 1A). GFP::Ub localizes to MOs which is consistent with antibody staining results using anti-ubiquitin and anti-MO antibodies (Al Rawi et al., 2011; Hajjar et al., 2014; Sato et al., 2018). In all images shown throughout, embryos are oriented with the sperm entry point (future posterior end of the embryo) towards the right and the anterior end towards the left. All embryos shown throughout are the result of self-fertilization in hermaphrodites with the exception of matings with males that are used later in this study when tracking paternal mitochondria in the zygote.

RNAi knockdown of individual UBCs did not affect GFP::Ub localization to MOs (Figure 1B). However, in worms with simultaneous knockdown of *ubc-18* and *ubc-16* we observed a 50% reduction in 1 cell embryos with GFP::Ub surrounding the paternal DNA (Figure 1C and 1D). Although 50% of embryos showed complete loss of GFP::Ub structures surrounding the paternal DNA, many of the remaining embryos showed reduced GFP::Ub signal around the DNA. Even though the levels were reduced, these embryos were scored as positive for GFP::Ub.

Since knockdown of either UBC alone did not affect GFP::Ub localization, this indicates that *ubc-18* and *ubc-16* are both involved in ubiquitination of MOs. The two UBCs are not closely related (24% identity). UBC-16 is 59% identical to the human enzyme UBE2W which is involved in monoubiquitination at the N terminus of proteins (Scaglione et al., 2013; Tatham et al., 2013). UBC-18 is 59% identical to human UBE2L3 (UbcH7) and has

been show to behave similar to its human homolog biochemically (Dove et al., 2017). UBC-18 and its human homolog partner with HECT or RBR E3 ubiquitin ligases during ubiquitination reactions (Dove et al., 2016).

The loss of GFP::Ub in the embryo is an actual reduction in ubiquitination of MOs and not a loss of MOs themselves as shown via antibody stains with an anti-MO antibody (Figure 2). That we did not see complete loss of MO ubiquitination could indicate either that the RNAi knockdown of UBCs was not complete or that other UBCs are also involved.

Ubiquitination is known to promote the autophagic clearance of organelles (Kim et al., 2008; Kirkin et al., 2009). In order to understand how ubiquitination of MOs influences the fate of those organelles, we followed their persistence throughout early cell divisions. Using the MO antibody, 1CB4, we counted MO numbers in early stage embryos. In normal *C. elegans* embryogenesis, meiosis I is completed just after fertilization and the first polar body is formed. Immediately after meiosis I, meiosis II ensues, and a second polar body is released. It takes about 20-30 minutes to complete both meiotic divisions. Following meiosis, the maternal and paternal DNA decompact and form pronuclei which migrate toward the middle of the zygote and then engage in the first mitosis. This process is shown in Figure 1A. MO numbers and localization are dynamic during the first several cell divisions. During meiosis I, 16-20 MOs surround the paternal DNA. In control embryos, MO numbers drop by about 50% between the 1 cell and 2 cell stage (Figure 2). However, MO numbers remain constant in *ubc-18/ubc-16* knockdown embryos between the 1 cell and 2 cell stages. This result suggests that ubiquitination is required for the early removal of MOs. In control embryos, MO numbers drop again during the transition from the 2 cell to 4 cell stage. However, MO numbers remain higher than control in the *ubc-18/ubc-16* knockdown embryos (Figure 2A and 2B). RNAi of either *ubc-18* or *ubc-16* alone did not affect the number of MOs. As a positive control, we did RNAi knockdown of *lgg-1/lgg-2* (the LC3/GABARAP homologs in *C. elegans*) which should eliminate autophagy in the early embryo. As expected, this treatment caused a persistence of MOs. These results suggest that ubiquitination of MOs is important for their removal in the early embryo.

Two types of ubiquitin chains have been identified on MOs: lysine 48 (K48) and lysine 63 (K63) (Al Rawi et al., 2011; Hajjar et al., 2014). K48 chains are only present on MOs for a few minutes during meiosis I, while K63 chains are detected throughout the early cleavages (Hajjar et al., 2014). After identifying two UBCs responsible for ubiquitinating MOs, we wanted to determine if each UBC was responsible for a specific ubiquitin chain. Using chain specific antibodies, we found that the presence of K63 chains was not affected by knockdown of either UBC individually or simultaneously (supplemental Figure 1). However, K48 chains were only present in 28% of *ubc-18(RNAi)* meiosis I embryos versus 95% of control embryos (Figure 3B). Mutant embryos showed expected MO clustering around the paternal DNA even without K48 chains (Figure 3A). K48 staining is also decreased in embryos treated with combined *ubc-18/ubc-16(RNAi)* (Figure 3A, B). On the other hand, *ubc-16(RNAi)* embryos did not show reduced K48 chains (Figure 3A, B). Therefore, the loss of K48 chains seen in the *ubc-18/ubc-16(RNAi)* is likely due to the absence of *ubc-18*. The same results were seen when a *ubc-18* mutant was used (*ku354*) instead of RNAi (supplemental Figure 2). These results indicate that *ubc-18* is required for the formation of

K48 ubiquitin chains on MOs immediately after fertilization. Since the *ubc-18(RNAi)* only affects K48 ubiquitin chains and the double RNAi (*ubc-18/ubc-16*) reduces overall localization of ubiquitin to MOs (Figure 1D) but does not appreciably affect the presence of K63 chains, this suggests that monoubiquitination or some other type of ubiquitin chain predominates on MOs. Since the human homolog of *ubc-16*, UBE2W, has been show to ubiquitinate at the N-terminus of substrates (Scaglione et al., 2013; Tatham et al., 2013), it would be interesting to determine if there are N-terminal chains present on MOs. The development of new tools in the ubiquitin field will hopefully aid in the pursuit of this interesting question.

Proteasome recruitment affects the elimination of membranous organelles but not autophagosome formation

K48 polyubiquitin chains can serve as a signal for recognition by the proteasome and subsequent degradation (López-Mosqueda and Dikic, 2014; Thrower et al., 2000). Proteasomes have been detected on MOs during meiosis I during the same time period when K48 ubiquitin chains are present (Hajjar et al., 2014). We wanted to determine if loss of K48 chains would affect recruitment of proteasomes to MOs. For this, we used a transgenic worm expressing a GFP-tagged proteasomal subunit RPT-1. In vector treated embryos, RPT-1::GFP localizes to the region around the sperm DNA during meiosis I consistent with previously reported localization of the proteasome to MOs (Al Rawi et al., 2011; Hajjar et al., 2014). As anticipated, proteasomal localization was diminished in *ubc-18(RNAi)* (Figure 4A, B). These data are consistent with the scenario where K48 chains are involved in proteasome recruitment to MOs after fertilization.

Rpn10 and Rad23 are proteins subunits of the regulatory particle of the proteasome known to interact with polyubiquitin chains and are thought to recruit ubiquitinated proteins to the proteasome for degradation (Zhang et al., 2009). The *C. elegans* homologs of these ubiquitin receptor proteins, *rpn-10* and *rad-23*, are not essential as knockdowns of these genes yields wild type embryonic viability (supplemental Figure 3). We wondered whether one of these ubiquitin receptors might be involved in recruiting the proteasome to the K48 chains on the MOs. When each of these were knocked down via RNAi, localization of proteasome to MOs was disrupted (Figure 4A and 4B) suggesting that both of these ubiquitin receptors are involved in recruiting the proteasome to MOs.

The Xue lab has reported that *rpn-10* and *rad-23* ubiquitin receptors are involved in the removal of paternal mitochondrial DNA (Zhou et al., 2011). Therefore, we wanted to test whether MO removal was affected when these were knocked down. RNAi of *rpn-10* and *rad-23* increased MO numbers in the 2 to 8 cell stages (Figure 2A and 2B). Since removal of MOs is believed to occur via autophagy, we decided to observe whether autophagosome formation is disrupted in proteasome ubiquitin receptor knockdowns. Using an LGG-1::GFP transgenic worm we tracked the formation of vesicles in 1 cell embryos. LGG-1 vesicles begin to form around the MOs and paternal mitochondria during meiosis II (Al Rawi et al., 2011; Djeddi et al., 2015). LGG-1::GFP in embryos appears either as small dispersed dots (puncta) or larger figures which are clustered around the sperm DNA (vesicle clusters). In several cases, these larger spots appear hollow consistent with autophagosome vesicle

formation. Control embryos showed a large percentage of embryos containing vesicle clusters (Figure 5A). RNAi knockdowns of *rpn-10* and *rad-23* do not disrupt the formation of the vesicle clusters (Figure 5E and 5F). Knockdown of *atg-7*, the E1 enzyme for the autophagy pathway, eliminated autophagosome vesicle formation (Figure 5B). Also, *ubc-18(RNAi)* embryos showed a reduced number of LGG-1 vesicles (Figure 5C and 5D). However, a greater reduction in the number of LGG-1 vesicles was observed in the double knockdown of *ubc-18(RNAi)* with *ubc-16(RNAi)* (Figure 5D). These results suggest that ubiquitination of MOs, but not proteasome recruitment contributes to autophagosome formation in 1 cell embryos.

This paradoxical result that *rpn-10* and *rad-23* knockdowns do not affect autophagosome formation but do lead to persistence of the MOs suggests that proteasome is required for an event that occurs after LGG-1 recruitment. Perhaps the proteasome is involved in the degradation or processing of some component of the autophagosome that leads to its fusion with the lysosome. The process of autophagosome-lysosome fusion involves a number of proteins for the transport, tethering, and fusion of these two vesicles (Nakamura and Yoshimori, 2017). Our data suggests that in the case of paternal mitochondria elimination, proteasomal function is involved in this process.

Removal of paternal mitochondria in the 1 cell embryo requires MO ubiquitination

Our finding that the proteasome is involved in MO elimination lead us to wonder whether the proteasome is also involved in the elimination of paternal mitochondria. Zhou et al. (2011) had shown that *rpn-10* and *rad-23* knockdown leads to persistence of paternal mitochondrial DNA. We wanted to examine cytologically if paternal mitochondria persist. There is evidence from mammalian cell culture that the proteasome plays a role in activating mitophagy components to destroy damaged mitochondria in the canonical mitophagy pathway (Chan et al., 2011; Gegg and Schapira, 2011; Tanaka et al., 2010; Wang et al., 2016). In order to test whether the proteasome is also involved in elimination of paternal mitochondria in *C. elegans*, we examined persistence of paternal mitochondria in *rpn-10(RNAi)* or *rad-23(RNAi)* embryos. In both cases, paternal mitochondria were retained in multi-cellular embryos (Figure 4C and 4D). This finding suggests that the proteasome activity and/or its localization to MOs is important for the mitophagy of paternal mitochondria.

An interesting discrepancy between the emerging stories of paternal mitochondria elimination in *C. elegans* versus mammalian species is the role of ubiquitination. Reports from mammalian species suggest that paternal mitochondria are themselves ubiquitinated (Sutovsky et al., 1999, 2000). However, in C. *elegans* the paternal mitochondria themselves are not ubiquitinated but the MOs are. In one report, it was suggested that the mitochondria are ubiquitinated at a low level in *C. elegans* embryos (Sato et al., 2018), but we have been unable to confirm this result in our lab. Therefore, we were interested to investigate how ubiquitination of MOs affects the elimination of paternal mitochondria. The initial model put forth for removal of paternal mitochondria in *C. elegans* proposed that ubiquitination of MOs would recruit autophagosome membranes that would also engulf the paternal mitochondria since they were clustered together (Al Rawi et al., 2011; Sato and Sato, 2011).

Thus, ubiquitination of MOs should contribute to elimination of paternal mitochondria. Since we have now identified a scenario where MO ubiquitination is reduced, we tested whether paternal mitochondria elimination is affected. Mitotracker labeled males were mated with control or RNAi treated hermaphrodites that express mCherry tagged histone 2B in the germline. After the matings, embryos were extracted from the mated hermaphrodites and imaged with confocal microscopy. As predicted by the model, embryos with simultaneous knockdown of *ubc-18/ubc-16* show persistence of mitochondria at the 2 cell stage (Figure 6A and 6C). Unexpectedly, the same persistence of paternal mitochondria is seen in *ubc-18(RNAi)* (Figure 6A and 6C). This result suggests that perhaps it is not overall ubiquitination, but K48 ubiquitination of the MOs that is important for the removal of paternal mitochondria.

RNAi of *lgg-1/lgg-2* was included as a control that should inhibit all autophagy. Indeed, under those conditions, paternal mitochondria persisted into the multicellular stages (Figure 6C). In contrast, RNAi of *ubc-18* only affected paternal mitochondria removal at the 2 cell stage. Paternal mitochondria were eventually removed in *ubc-18(RNAi)* and the numbers were similar to wild type embryos at the 4 cell stage and beyond. These results indicate that there are redundant but temporally distinct pathways for removing paternal mitochondria. Ubiquitination by *ubc-18* appears to be involved in removal of paternal mitochondria immediately after fertilization during the meiotic divisions and the first mitosis.

fndc-1 *is required for removal of paternal mitochondria after the 2 cell stage*

In order to investigate ubiquitin independent pathways for paternal mitochondria elimination, we chose to look at *fndc-1.* During periods of hypoxia, mitophagy can be driven by the mitochondrial receptor FUNDC1 independently of ubiquitination (Liu et al., 2012). *fndc-1* is the *C. elegans* homolog of this gene. In a partner report from Im *et al*, it is shown that *fndc-1* is constitutively expressed in sperm and could potentially serve as a mitophagy receptor involved in paternal mitochondria elimination (reference Im et al. partner paper). *fndc-1* mutant males were labelled with Mitotracker and mated with N2 hermaphrodites and paternal mitochondria numbers were assessed. Figure 6C shows embryos at the 2 cell, 4 cell and 8-12 cell stage. Embryos fertilized by *fndc-1* males showed persistence of paternal mitochondria in 8-12 cell embryos. However, the number of paternal mitochondria during the 2 cell stage in mutants was similar to wild type (Figure 6B). Thus, *fndc-1* may be part of a pathway for paternal mitochondria elimination that is independent of MO ubiquitination. Therefore, paternal mitochondria that escape elimination via engulfment with ubiquitnated MOs could later be eliminated via the *fndc-1* pathway (Figure 7).

Discussion:

Strict maternal inheritance of the mitochondria is observed in most metazoans (Hutchison et al., 1974). In mice, having two different types of mitochondria (heteroplasmy) negatively affects their cognitive abilities (Sharpley et al., 2012). Perhaps due to the negative consequences of heteroplasmy, organisms have evolved mechanisms to eliminate paternal mitochondria that enter the oocyte during fertilization. Selective autophagy is recognized as a probable mechanism involved in the paternal mitochondria elimination. Therefore, our

goal was to establish whether ubiquitination was selecting MOs for degradation and driving simultaneous elimination of paternal mitochondria.

Our results indicate that MO ubiquitination is required for the elimination of paternal mitochondria that occurs shortly after fertilization in the 1 cell embryo (Figure 7). However, ubiquitination is not required for the elimination of paternal mitochondria that occurs past the 2 cell stage. Interestingly, our results suggest that it is K48-linked ubiquitin chains rather than K63-linked chains that are more crucial for paternal mitochondria elimination. This is based on the findings that knockdown of *ubc-18* removes K48 chains from MOs and also causes paternal mitochondria to persist at the 2 cell stage. The finding that K63 chains are not critical for the elimination of MOs or mitochondria is contrary to a model where K63 chains are critical in the recruitment of autophagosomal membranes during paternal organelle elimination. Our results suggest that there may be other ubiquitin chains that can act to recruit autophagsomes.

Knockdown of *ubc-18* alone does not cause persistence of MOs, but in the double knockdown (*ubc-18/ubc-16*) LGG-1 recruitment is reduced and the MOs do persist. Thus, some UBC-18 activity is important for linking the autophagy of MOs with the autophagy of the paternal mitochondria. This could involve K48 chains and recruitment of the proteasome since *rpn-10* and *rad-23* knockdowns also cause persistence of paternal mitochondria. Overall, our data are consistent with a model where UBC-18 adds K48 chains which then recruit the proteasome which then leads to autophagosome maturation and inclusion of paternal mitochondria in the selective autophagy process (Figure 7). Ubiquitination by UBC-18 plus UBC-16 results in a variety of linkage types and is required for the recruitment of the autophagosome membranes and the elimination of MOs. It is possible that UBC-18 and UBC-16 are involved sequential ubiquitination of substrates as was seen with UBC-18 and UBC-3 (Dove et al., 2017).

Elimination of paternal mitochondria shares similarities with the canonical mitophagy pathway. In both cases, autophagy, ubiquitination, and fission-fusion pathways have been implicated (Sato and Sato, 2017). Interestingly, there does not seem to be evidence for the PINK/Parkin system in paternal mitochondria elimination in *C. elegans* (Sato et al., 2018). Since the paternal mitochondria themselves are not ubiquitinated in *C. elegans*, this is not surprising. Proteasome involvement is another common element between paternal mitochondria elimination and the canonical mitophagy pathway. In the canonical mitophagy pathway, the proteasome is believed to degrade mitofusion proteins through a p97 dependent mechanism, driven by Parkin induced ubiquitination of mitofusins (Gegg and Schapira, 2011; Tanaka et al., 2010). It has not yet been tested whether the mitofusions are the targets of proteasomal degradation in paternal mitophagy. Another report suggested that proteasome activity is required for the removal of paternal mitochondria following fertilization in mammals (Sutovsky et al., 2000). Our data support that two ubiquitin recognition subunits of the proteasome, *rpn-10* and *rad-23*, are required for the removal of both paternal mitochondria and MOs. These proteasomal subunits are required for early localization of the proteasome to MOs during meiosis I similar to the phenotype observed in *ubc-18(RNAi)* knockdowns. Since disruption of proteasome localization via knockdown of *ubc-18, rpn-10*, or *rad-23* correlates with persistence of paternal mitochondria, it is tempting to speculate

that proteasomal degradation of some component associated with either the MOs or the mitochondria is involved in selective autophagy of paternal mitochondria. This factor may be something required for autophagosome-lysosome fusion since the *rpn-10* and *rad-23* phenotypes show that LGG-1 recruitment is not affected, but that mitochondria and MOs persist in the embryo.

p97/VCP is a proteasome associated protein that aids in the process of ubiquitin mediated protein degradation (Stolz et al., 2011). p97 has also been shown to participate in membrane fusion and autophagosome maturation (Ju et al., 2009). It is possible that RPN-10 and RAD-23 could facilitate a link between the autophagsome and lysosome via their recruitment of p97. This scenario would explain why the loss of proteasome localization to MOs might interfere with their maturation into autophagolysosomes and the ultimate elimination of MOs and paternal mitochondria. In the absence of RPN-10 or RAD-23, p97 recruitment could be disrupted and autophagosome-lysosome fusion might not take place.

Our analysis of paternal mitochondria elimination in *C. elegans* points to the involvement of at least two pathways. Disruption of MO ubiquitination affects paternal mitochondria elimination that occurs very soon after fertilization (during the 1 cell stage). However, if mitochondria do persist during this period, they are ultimately eliminated by some the other pathway. Loss of function of *fndc-1* does not affect paternal mitochondria elimination during the 1 and 2 cell stages, but does affect paternal mitochondria elimination in the 4-8 cell stage. Thus, there are two redundant mechanisms for targeting paternal mitochondria for elimination: one that involves ubiquitination of the MOs and a second that involves a ubiquitin independent system and the FNDC-1 protein. Both pathways utilize the autophagy system to ultimately degrade the mitochondria. Further investigation into the interactions between these various components will provide a clearer understanding of how these organelles are tagged and eliminated.

Supplementary Material

Refer to Web version on PubMed Central for supplementary material.

Acknowledgements:

We would like to thank Keith Nehrke for supplying the KWN775 strain and Vincent Galy for helpful comments on the manuscript. We thank Steve L'Hernault for the 1CB4 antibody. We are grateful to members of the Boyd laboratory as well as David Nelson and Jason Jessen for input on the project. Some strains were provided by the CGC, which is funded by NIH Office of Research Infrastructure Programs (P40 OD010440). YL was supported from R01 HL127891. This work was supported by an NIH grant to LB: R15 HD083882.

References

Al Rawi S, Louvet-Vallee S, Djeddi A, Sachse M, Culetto E, Hajjar C, Boyd L, Legouis R, Galy V, 2011 Postfertilization autophagy of sperm organelles prevents paternal mitochondrial DNA transmission. Science 334, 1144–1147. [PubMed: 22033522]

Bjorkoy G, Lamark T, Brech A, Outzen H, Perander M, Overvatn A, Stenmark H, Johansen T, 2005 p62/SQSTM1 forms protein aggregates degraded by autophagy and has a protective effect on huntingtin-induced cell death. J Cell Biol 171, 603–614. [PubMed: 16286508]

Boyd L, Hajjar C, O'Connell K, 2011 Time-lapse microscopy of early embryogenesis in *Caenorhabditis elegans*. J Vis Exp.

Brenner S, 1974 The genetics of *Caenorhabditis elegans*. Genetics 77, 71–94. [PubMed: 4366476]

Chan DC, Schon EA, 2012 Eliminating mitochondrial DNA from sperm. Dev Cell 22, 469–470. [PubMed: 22421036]

Chan NC, Salazar AM, Pham AH, Sweredoski MJ, Kolawa NJ, Graham RL, Hess S, Chan DC, 2011 Broad activation of the ubiquitin-proteasome system by Parkin is critical for mitophagy. Hum Mol Genet 20, 1726–1737. [PubMed: 21296869]

Christensen DE, Brzovic PS, Klevit RE, 2007 E2-BRCA1 RING interactions dictate synthesis of mono- or specific polyubiquitin chain linkages. Nat Struct Mol Biol 14, 941–948. [PubMed: 17873885]

DeLuca SZ, O'Farrell PH, 2012 Barriers to male transmission of mitochondrial DNA in sperm development. Dev Cell 22, 660–668. [PubMed: 22421049]

Djeddi A, Al Rawi S, Deuve JL, Perrois C, Liu YY, Russeau M, Sachse M, Galy V, 2015 Sperm-inherited organelle clearance in *C. elegans* relies on LC3-dependent autophagosome targeting to the pericentrosomal area. Development 142, 1705–1716. [PubMed: 25922527]

Dove KK, Kemp HA, Di Bona KR, Reiter KH, Milburn LJ, Camacho D, Fay DS, Miller DL, Klevit RE, 2017 Two functionally distinct E2/E3 pairs coordinate sequential ubiquitination of a common substrate in. Proc Natl Acad Sci U S A 114, E6576–E6584. [PubMed: 28739890]

Dove KK, Stieglitz B, Duncan ED, Rittinger K, Klevit RE, 2016 Molecular insights into RBR E3 ligase ubiquitin transfer mechanisms. EMBO Rep 17, 1221–1235. [PubMed: 27312108]

Gatica D, Lahiri V, Klionsky DJ, 2018 Cargo recognition and degradation by selective autophagy. Nat Cell Biol 20, 233–242. [PubMed: 29476151]

Gegg ME, Schapira AH, 2011 PINK1-parkin-dependent mitophagy involves ubiquitination of mitofusins 1 and 2: Implications for Parkinson disease pathogenesis. Autophagy 7, 243–245. [PubMed: 21139416]

Geisler S, Holmstrom KM, Skujat D, Fiesel FC, Rothfuss OC, Kahle PJ, Springer W, 2010 PINK1/Parkin-mediated mitophagy is dependent on VDAC1 and p62/SQSTM1. Nat Cell Biol 12, 119–131. [PubMed: 20098416]

Hajjar C, Sampuda KM, Boyd L, 2014 Dual roles for ubiquitination in the processing of sperm organelles after fertilization. J BMC developmental biology 14, 6.

Husnjak K, Elsasser S, Zhang N, Chen X, Randles L, Shi Y, Hofmann K, Walters KJ, Finley D, Dikic I, 2008 Proteasome subunit Rpn13 is a novel ubiquitin receptor. Nature 453, 481–488. [PubMed: 18497817]

Hutchison CA 3rd, Newbold JE, Potter SS, Edgell MH, 1974 Maternal inheritance of mammalian mitochondrial DNA. Nature 251, 536–538. [PubMed: 4423884]

Huynh KK, Eskelinen EL, Scott CC, Malevanets A, Saftig P, Grinstein S, 2007 LAMP proteins are required for fusion of lysosomes with phagosomes. EMBO J 26, 313–324. [PubMed: 17245426]

Ju JS, Fuentealba RA, Miller SE, Jackson E, Piwnica-Worms D, Baloh RH, Weihl CC, 2009 Valosin-containing protein (VCP) is required for autophagy and is disrupted in VCP disease. J Cell Biol 187, 875–888. [PubMed: 20008565]

Kamath RS, Fraser AG, Dong Y, Poulin G, Durbin R, Gotta M, Kanapin A, Le Bot N, Moreno S, Sohrmann M, Welchman DP, Zipperlen P, Ahringer J, 2003 Systematic functional analysis of the *Caenorhabditis elegans* genome using RNAi. Nature 421, 231–237. [PubMed: 12529635]

Kim PK, Hailey DW, Mullen RT, Lippincott-Schwartz J, 2008 Ubiquitin signals autophagic degradation of cytosolic proteins and peroxisomes. Proc Natl Acad Sci U S A 105, 20567–20574. [PubMed: 19074260]

Kirkin V, Lamark T, Sou YS, Bjorkoy G, Nunn JL, Bruun JA, Shvets E, McEwan DG, Clausen TH, Wild P, Bilusic I, Theurillat JP, Overvatn A, Ishii T, Elazar Z, Komatsu M, Dikic I, Johansen T, 2009 A role for NBR1 in autophagosomal degradation of ubiquitinated substrates. Mol Cell 33, 505–516. [PubMed: 19250911]

Liu L, Feng D, Chen G, Chen M, Zheng Q, Song P, Ma Q, Zhu C, Wang R, Qi W, Huang L, Xue P, Li B, Wang X, Jin H, Wang J, Yang F, Liu P, Zhu Y, Sui S, Chen Q, 2012 Mitochondrial outer-membrane protein FUNDC1 mediates hypoxia-induced mitophagy in mammalian cells. Nat Cell Biol 14, 177–185. [PubMed: 22267086]

López-Mosqueda J, Dikic I, 2014 Deciphering functions of branched ubiquitin chains. J Cell 157, 767–769.

Matsumoto G, Wada K, Okuno M, Kurosawa M, Nukina N, 2011 Serine 403 phosphorylation of p62/SQSTM1 regulates selective autophagic clearance of ubiquitinated proteins. Mol Cell 44, 279–289. [PubMed: 22017874]

Nakamura S, Yoshimori T, 2017 New insights into autophagosome-lysosome fusion. J Cell Sci 130, 1209–1216. [PubMed: 28302910]

Politi Y, Gal L, Kalifa Y, Ravid L, Elazar Z, Arama E, 2014 Paternal mitochondrial destruction after fertilization is mediated by a common endocytic and autophagic pathway in Drosophila. Dev Cell 29, 305–320. [PubMed: 24823375]

Roberts TM, Pavalko FM, Ward S, 1986 Membrane and cytoplasmic proteins are transported in the same organelle complex during nematode spermatogenesis. J Cell Biol 102, 1787–1796. [PubMed: 3517007]

Rodrigo-Brenni MC, Foster SA, Morgan DO, 2010 Catalysis of lysine 48-specific ubiquitin chain assembly by residues in E2 and ubiquitin. Mol Cell 39, 548–559. [PubMed: 20797627]

Rual JF, Ceron J, Koreth J, Hao T, Nicot AS, Hirozane-Kishikawa T, Vandenhaute J, Orkin SH, Hill DE, van den Heuvel S, Vidal M, 2004 Toward improving *Caenorhabditis elegans* phenome mapping with an ORFeome-based RNAi library. Genome Res 14, 2162–2168. [PubMed: 15489339]

Sato K, Sato M, 2017 Multiple ways to prevent transmission of paternal mitochondrial DNA for maternal inheritance in animals. J Biochem 162, 247–253. [PubMed: 28981751]

Sato M, Sato K, 2011 Degradation of paternal mitochondria by fertilization-triggered autophagy in *C. elegans* embryos. Science 334, 1141–1144. [PubMed: 21998252]

Sato M, Sato K, Tomura K, Kosako H, Sato K, 2018 The autophagy receptor ALLO-1 and the IKKE-1 kinase control clearance of paternal mitochondria in *Caenorhabditis elegans*. Nat Cell Biol 20, 81–91. [PubMed: 29255173]

Scaglione KM, Basrur V, Ashraf NS, Konen JR, Elenitoba-Johnson KS, Todi SV, Paulson HL, 2013 The ubiquitin-conjugating enzyme (E2) Ube2w ubiquitinates the N terminus of substrates. J Biol Chem 288, 18784–18788. [PubMed: 23696636]

Sharpley MS, Marciniak C, Eckel-Mahan K, McManus M, Crimi M, Waymire K, Lin CS, Masubuchi S, Friend N, Koike M, Chalkia D, MacGregor G, Sassone-Corsi P, Wallace DC, 2012 Heteroplasmy of mouse mtDNA is genetically unstable and results in altered behavior and cognition. Cell 151, 333–343. [PubMed: 23063123]

Soss SE, Klevit RE, Chazin WJ, 2013 Activation of UbcH5c~Ub is the result of a shift in interdomain motions of the conjugate bound to U-box E3 ligase E4B. Biochemistry 52, 2991–2999. [PubMed: 23550736]

Stiernagle T, 2006 Maintenance of *C. elegans*. WormBook, 1–11.

Stolz A, Hilt W, Buchberger A, Wolf DH, 2011 Cdc48: a power machine in protein degradation. Trends Biochem Sci 36, 515–523. [PubMed: 21741246]

Sutovsky P, McCauley TC, Sutovsky M, Day BN, 2003 Early degradation of paternal mitochondria in domestic pig (Sus scrofa) is prevented by selective proteasomal inhibitors lactacystin and MG132. Biol Reprod 68, 1793–1800. [PubMed: 12606393]

Sutovsky P, Moreno RD, Ramalho-Santos J, Dominko T, Simerly C, Schatten G, 1999 Ubiquitin tag for sperm mitochondria. Nature 402, 371–372. [PubMed: 10586873]

Sutovsky P, Moreno RD, Ramalho-Santos J, Dominko T, Simerly C, Schatten G, 2000 Ubiquitinated sperm mitochondria, selective proteolysis, and the regulation of mitochondrial inheritance in mammalian embryos. Biol Reprod 63, 582–590. [PubMed: 10906068]

Tanaka A, Cleland MM, Xu S, Narendra DP, Suen DF, Karbowski M, Youle RJ, 2010 Proteasome and p97 mediate mitophagy and degradation of mitofusins induced by Parkin. J Cell Biol 191, 1367–1380. [PubMed: 21173115]

Tatham MH, Plechanovová A, Jaffray EG, Salmen H, Hay RT, 2013 Ube2W conjugates ubiquitin to α-amino groups of protein N-termini. Biochem J 453, 137–145. [PubMed: 23560854]

Thrower JS, Hoffman L, Rechsteiner M, Pickart CM, 2000 Recognition of the polyubiquitin proteolytic signal. EMBO J 19, 94–102. [PubMed: 10619848]

Vittal V, Wenzel DM, Brzovic PS, Klevit RE, 2013 Biochemical and structural characterization of the ubiquitin-conjugating enzyme UBE2W reveals the formation of a noncovalent homodimer. Cell Biochem Biophys 67, 103–110. [PubMed: 23709311]

Wang Y, Zhang Y, Chen L, Liang Q, Yin XM, Miao L, Kang BH, Xue D, 2016 Kinetics and specificity of paternal mitochondrial elimination in *Caenorhabditis elegans*. Nat Commun 7, 12569. [PubMed: 27581092]

Yoo S-M, and Jung Y-K, 2018 A Molecular Approach to Mitophagy and Mitochondrial Dynamics. Mol Cells 41, 18–26. [PubMed: 29370689]

Zhang D, Chen T, Ziv I, Rosenzweig R, Matiuhin Y, Bronner V, Glickman MH, Fushman D, 2009 Together, Rpn10 and Dsk2 can serve as a polyubiquitin chain-length sensor. Mol Cell 36, 1018–1033. [PubMed: 20064467]

Zhou Q, Li H, Li H, Nakagawa A, Lin JL, Lee ES, Harry BL, Skeen-Gaar RR, Suehiro Y, William D, Mitani S, Yuan HS, Kang BH, Xue D, 2016 Mitochondrial endonuclease G mediates breakdown of paternal mitochondria upon fertilization. Science 353, 394–399. [PubMed: 27338704]

Zhou Q, Li H, Xue D, 2011 Elimination of paternal mitochondria through the lysosomal degradation pathway in *C. elegans*. Cell Res 21, 1662–1669. [PubMed: 22105480]

Highlights

- in *C. elegans, ubc-18* and *ubc-16* are ubiquitin conjugating enzymes required for ubiquitination of paternal membraneous organelles (MOs) after fertilization and for the recruitment of autophagosomes to the MOs
- ubiquitination of the MOs is required for the elimination of paternal mitochondria that occurs during the first cell cycle
- *ubc-18* is required for K48 polyubiquitin chains on MOs
- proteasome recruitment to MOs depends on both K48 ubiquitination and the ubiquitin receptors, *rpn-10* and *rad-23*
- when proteasome localization to MOs is disrupted, autophagosome membranes still form around the MOs, but the paternal mitochondria persist
- elimination paternal mitochondria after the 2 cell stage occurs via a ubiquitin-independent mechanism involving *fndc-1*

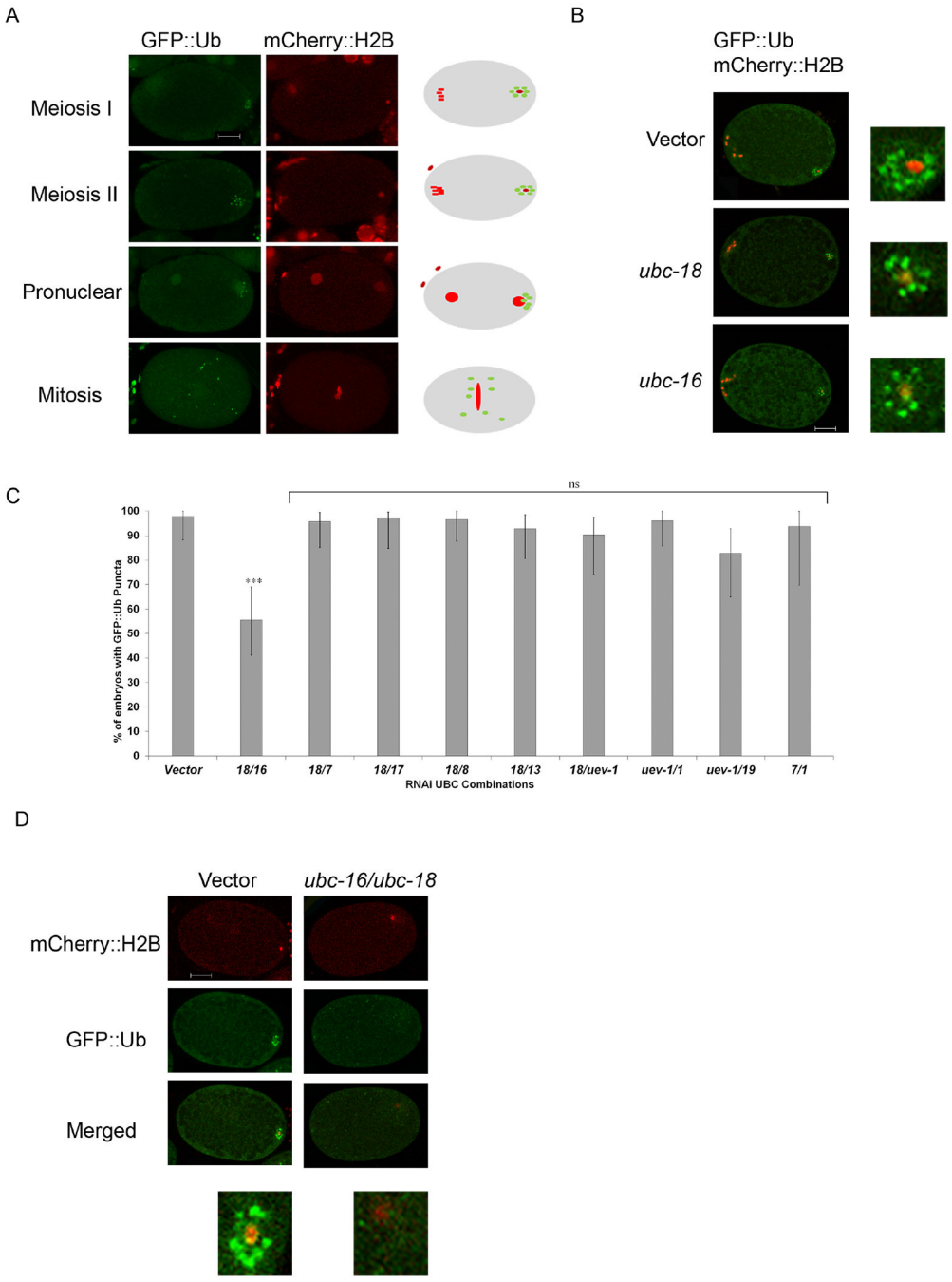

Figure 1. Simultaneous knockdown of *ubc-18* and *ubc-16* reduces ubiquitination of membraneous organelles.

Transgenic *C. elegans* embryos expressing GFP::Ub and mCherry::H2B were used to track the ubiquitination of MOs after RNAi knockdown of individual UBCs and double UBC combinations. **(A)** Wild type (vector control) embryos show the normal distribution of GFP::Ub following fertilization. The cartoon embryos to the right depict the characteristic pattern of GFP::Ub (green) and histone (red). In meiosis I and meiosis II embryos, GFP::Ub is concentrated on the MOs and localizes around the sperm DNA in the posterior region of

the embryo (posterior is to the right). During pronuclear formation and pronuclear movement, the MOs remain ubiquitinated and become more dispersed in the embryo. During mitosis, the MOs are dispersed throughout with a tendency to localize near the midline of the embryo. **(B)** Embryos from worms fed RNAi bacteria of *ubc-16* and *ubc-18* singly did not show a reduction in GFP::Ub surrounding the paternal DNA. Embryos shown are meiosis I or meiosis II embryos. **(C)** RNAi screen of double knockdown of UBCs. The graph represents the top 9 hits from the UBC combination screen. All other RNAi combinations showed GFP::Ub around sperm DNA in more than 80% of embryos. Simultaneous knockdown of *ubc-18* and *ubc-16* was the most promising result from the screen. The double knockdown showed a 40% reduction in one cell embryos with GFP::Ub vesicles. A total of 20 embryos were observed for each condition and statistical differences were determined using a two tailed z test. ***$p < 0.0001$ **(D)** Representative embryos from the *ubc-18/ubc-16* knockdown. Paternal DNA in embryos treated with *ubc-18* and *ubc-16* RNAi were not surrounded with GFP::Ub vesicles as is typically seen in empty vector treated worms. Scale bars 10 μm.

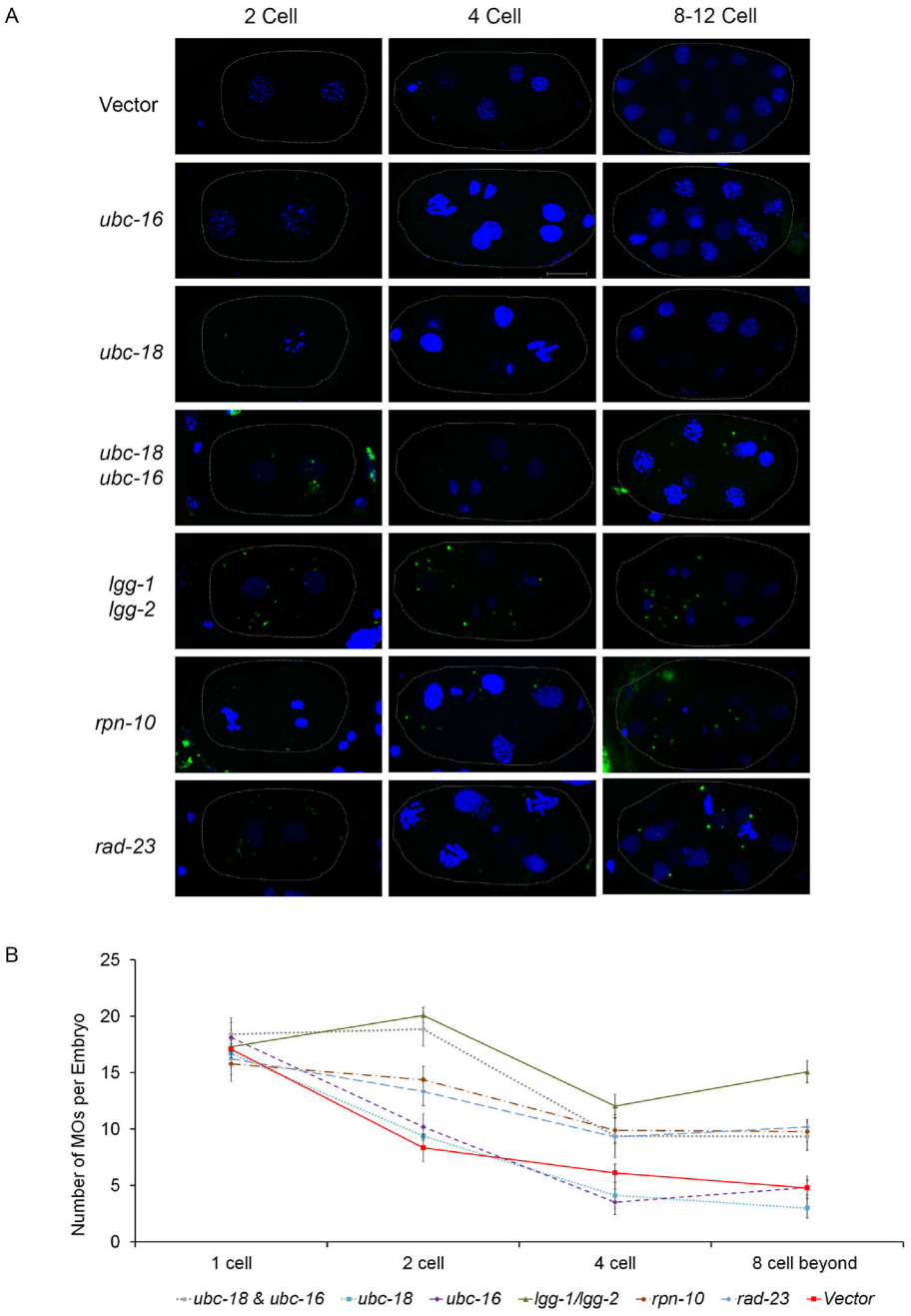

Figure 2. Reduction in MO ubiquitination correlates with a delay in their removal.

Embryos stained with an antibody that recognizes MOs were imaged and analyzed for the number of MOs per embryo. **(A)** Representative embryos from control and RNAi treatments. Maximum intensity *z*-projections of confocal images of embryos stained for MOs using the 1CB4 antibody (green) and DAPI for DNA (blue). In the vector control, MO numbers are reduced in 4- and 8-cell embryos. This reduction is not seen after RNAi treatment for *ubc-18/16* or *lgg-1/2*. Scale bar 10 μm. **(B)** MOs were counted in 10 embryos for each stage. Error bars in the graph represent the mean ± s.e.m. RNAi knockdowns were compared to

vector control and significant differences between were determined by unpaired *t* test. *ubc-18/ubc-16* knockdown treatment had a $p<0.001$, *lgg-1/2, rpn-10* and *rad-23* had a $p<0.0001$. *ubc-18* and *ubc-16* treatments were not statistically different from the control.

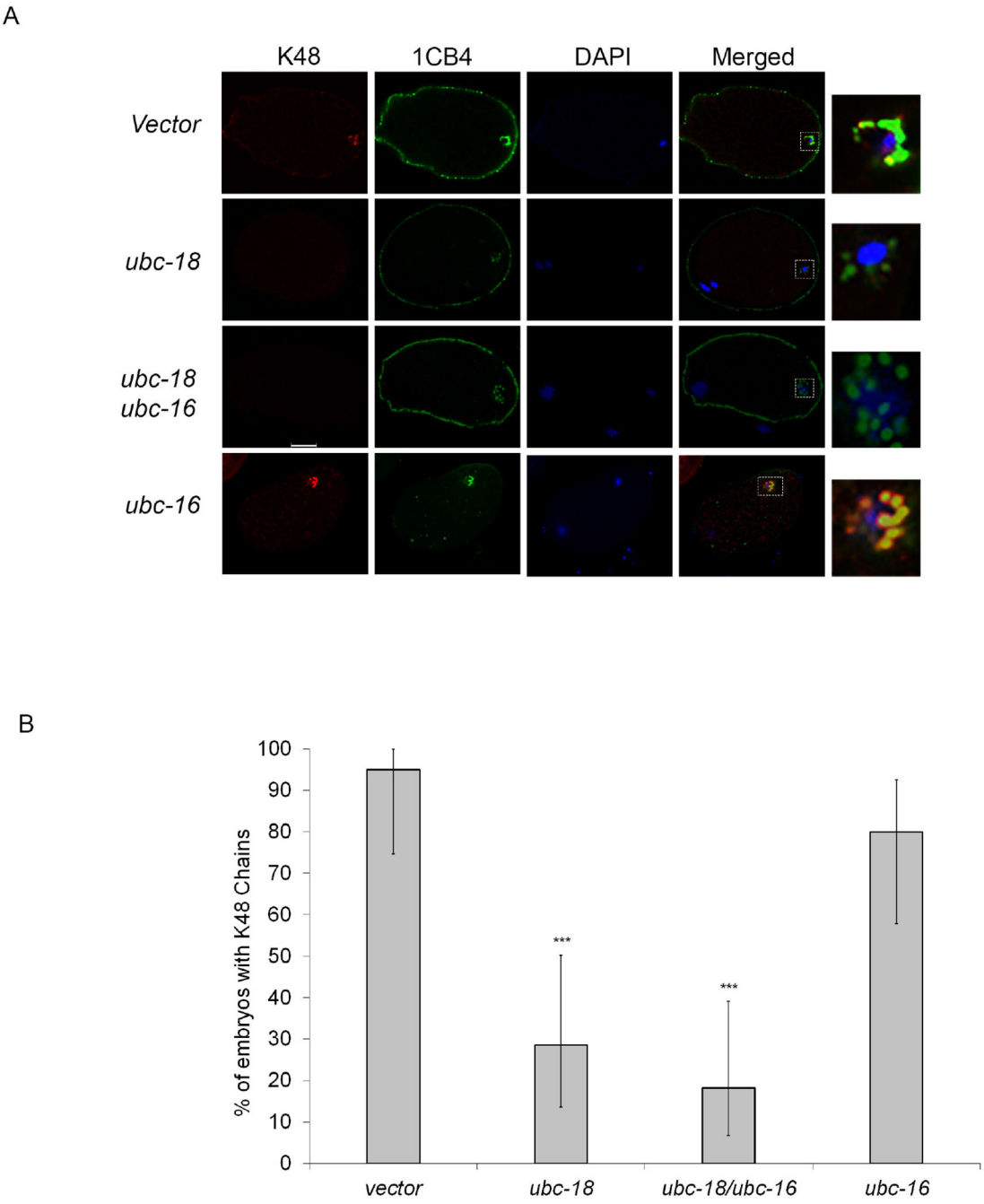

Figure 3. *ubc-18* is required for K48 ubiquitin chains on MOs during Meiosis I.

(A) N2, *ubc-18(RNAi), ubc-16(RNAi)* and *ubc-18/ ubc-16(RNAi)* embryos were stained with K48 chain specific and 1CB4 antibodies. In control embryos, K48 chains colocalize with MOs during meiosis I. This colocalization is disrupted after *ubc-18* RNAi. Scale bar 10 μm. **(B)** K48 chains were observed in 95% of control embryos, but only 28% of *ubc-18 (RNAi)* embryos. For each treatment 20 meiosis I embryos were observed. Statistical significance was calculated by a Fisher's Exact test: ***$p < 0.001$. Error bars represent 95% confidence intervals.

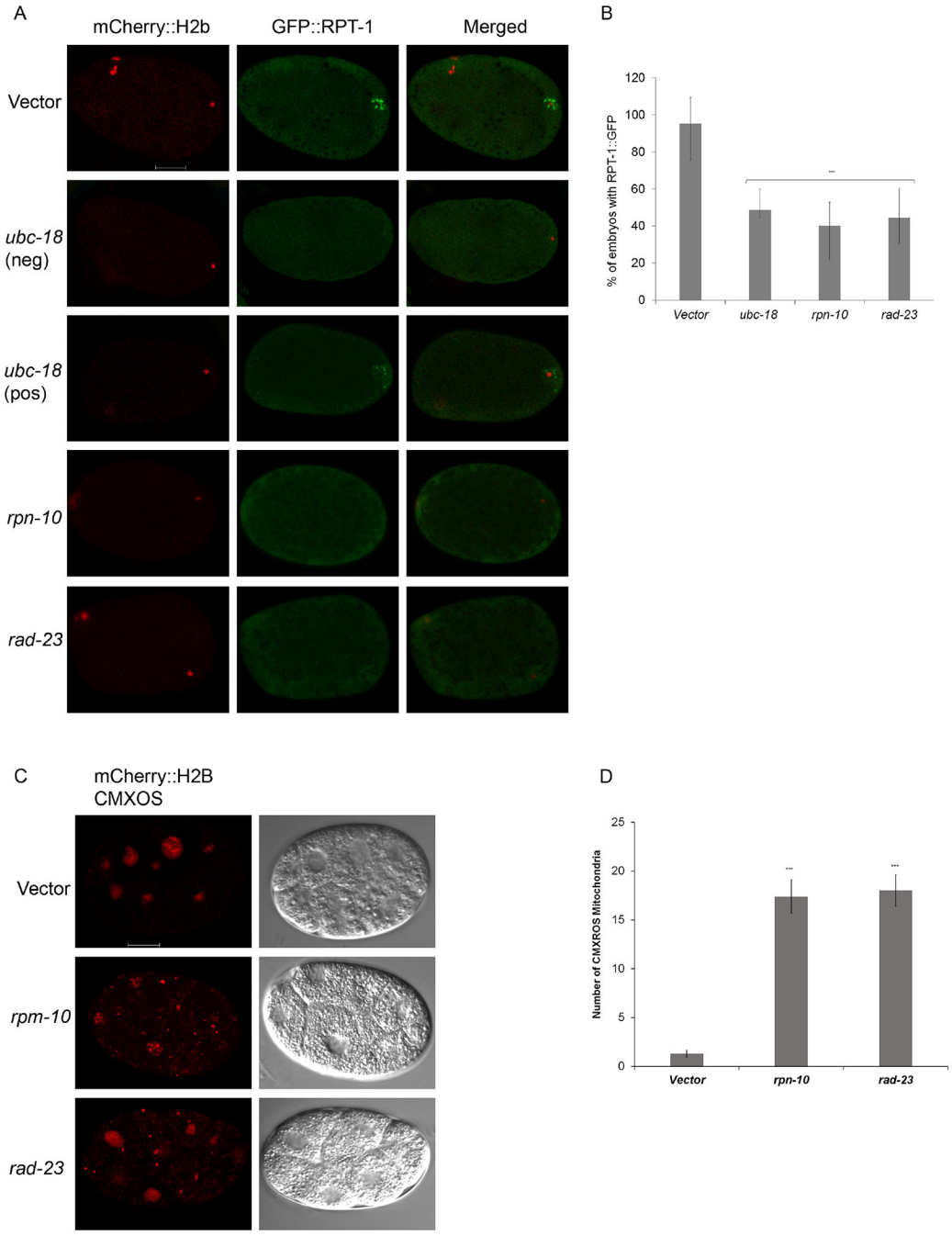

Figure 4. Proteasome recruitment requires *ubc-18, rpn-10,* and *rad-23*.

(A) Transgenic worms expressing mCherry::H2B and RPT-1::GFP fusion were treated with either vector, *ubc-18, rad-23*, or *rpn-10* RNAi. In vector treated meiosis I embryos, RPT-1::GFP localizes to the region around the sperm DNA. RNAi of *ubc-18, rpn-10*, or *rad-23* reduces the amount of RPT-1::GFP localizing around the sperm DNA. One embryo that was scored as positive for GFP::RPT-1 puncta after *ubc-18(RNAi)* is also shown (third row). Even though the puncta are present, the level of GFP at those puncta is lower than that seen in the control. **(B)** In about half of the RNAi treated embryos early proteasome

recruitment was absent. 30 Meiosis I embryos per treatment were observed. Statistical significance was calculated by a Fisher's Exact test: ***$p < 0.001$. Error bars represent 95% confidence intervals. **(C)** Paternal mitochondria were tracked in 8-12 cell embryos using CMXROS labeled males. Embryos from *rpn-10* and *rad-23* knockdowns showed larger numbers of paternal mitochondria persisting in 2-12 cell embryos when compared to the control. Both paternal mitochondria (CMXROS) and maternal DNA (mCherry::H2B) appear red in these images. **(D)** Quantification of mitochondria from 8-10 cell embryos. 12 embryos per trial with a total of 2 trials. Data in the graph represent the mean ± s.e.m. Significant differences between embryos was determined by unpaired *t* test. ***p<000.1.

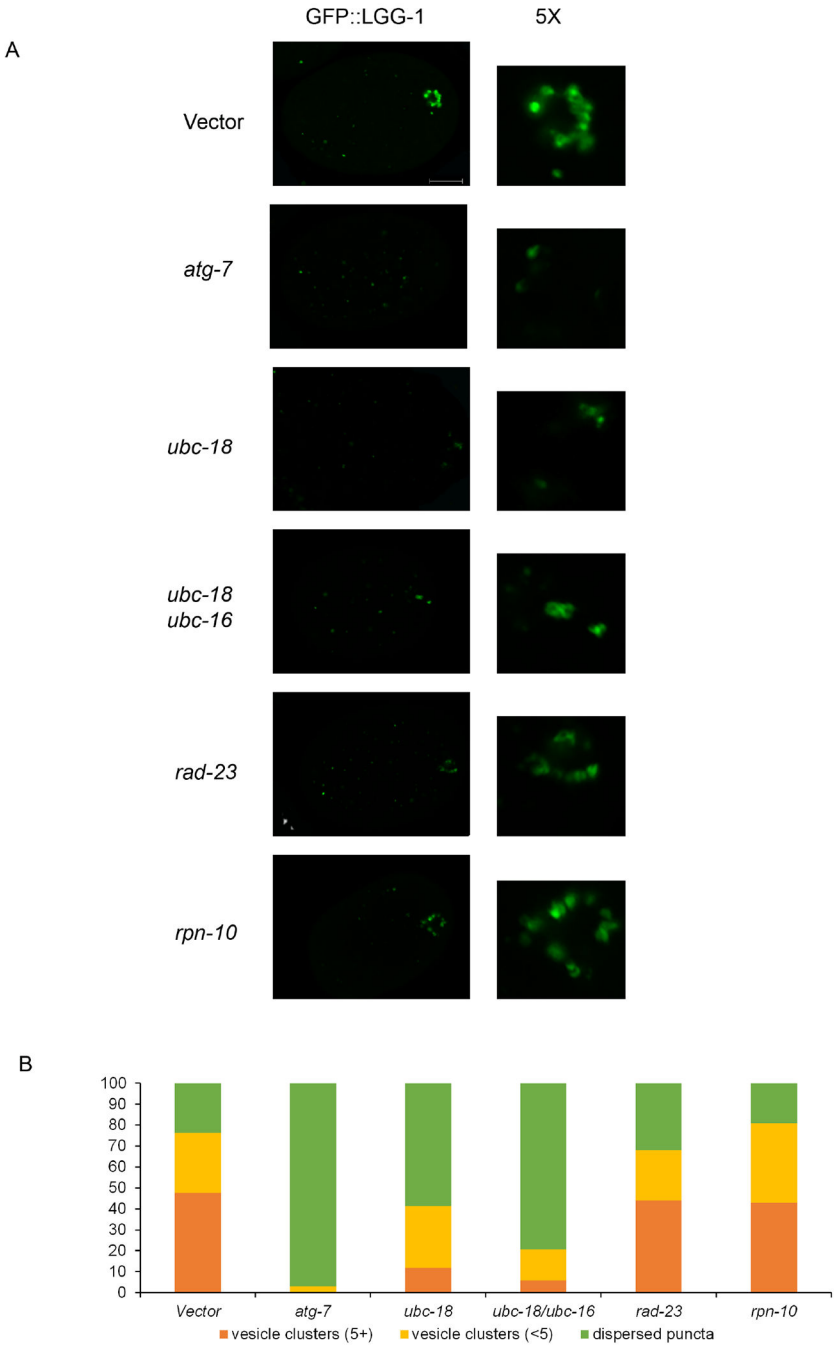

Figure 5. LGG-1 vesicle formation is reduced in *ubc-18/ubc-16* knockdown embryos but is not affected by *rpn-10* and *rad-23*.

LGG-1::GFP is used as a marker for autophagosome formation. **(A)** One-cell embryos were observed for the formation of autophagic vesicles. Control embryos showed several bright round GFP vesicles in the posterior region. LGG-1::GFP structures were characterized as either vesicle clusters which had large, often hollow spots clustering together. These were grouped into clusters of less than 5 (<5) or 5 or more (5+) vesicles. All embryos also had smaller dispersed puncta throughout. Embryos which only had dispersed puncta were categorized as “dispersed puncta”. Vesicles in embryos with proteasomal subunits

rpn-10(RNAi) and *rad-23(RNAi)* were similar to control in numbers and size. *atg-7(RNAi)* was used a positive control for autophagy disruption. Scale bar 10 μm. **(B)** The number of vesicle clusters in *ubc-18(RNAi)* and *ubc-18/ubc-16(RNAi)* was reduced. *ubc-18/ubc-16(RNAi)* embryos showed a more severe phenotype than *ubc-18 (RNAi)*. A total of 20 embryos were observed for each condition.

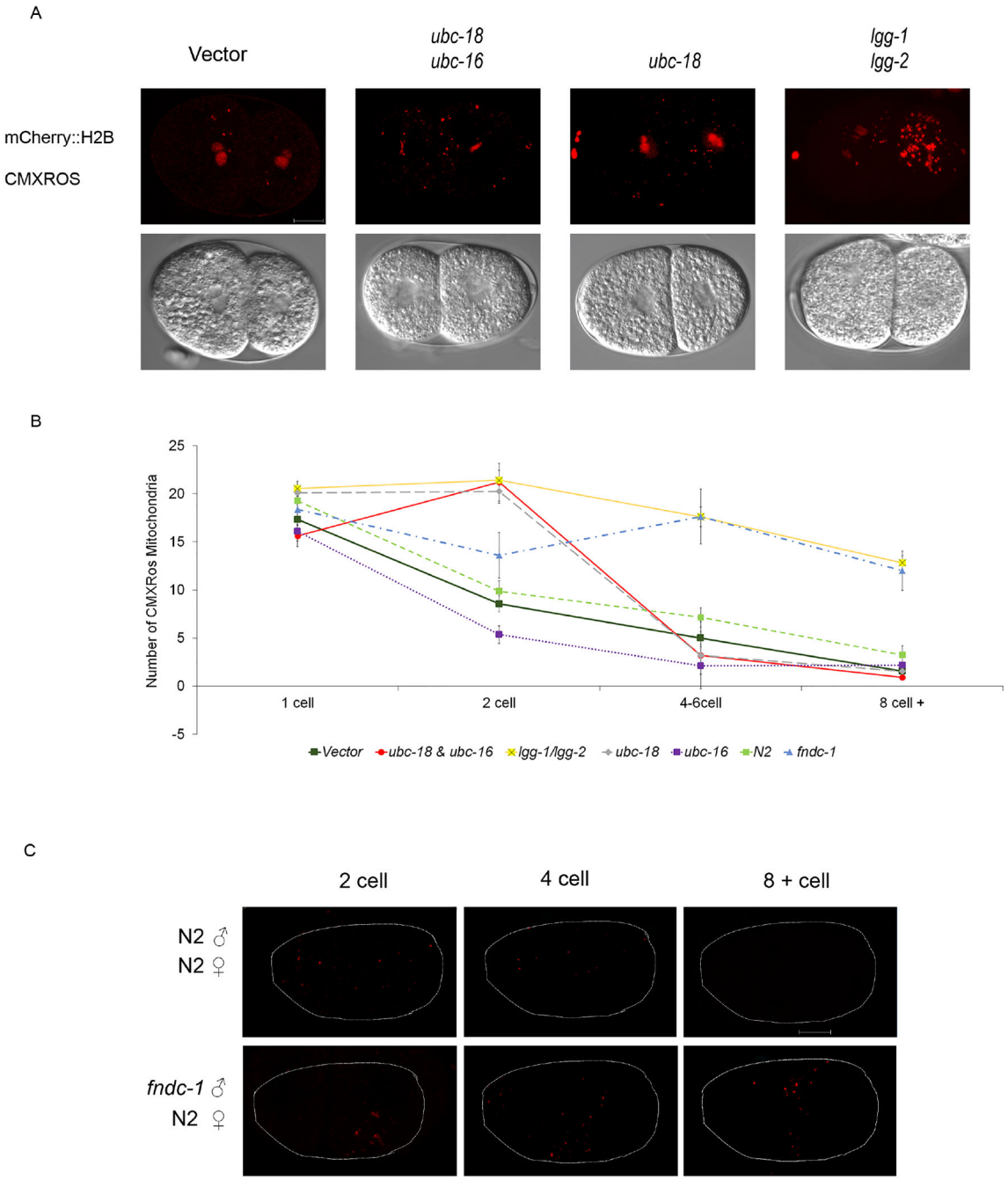

Figure 6. *ubc-18* is involved in early removal of paternal mitochondria.

Hermaphrodites expressing mCherry::H2B were mated with CMXROS soaked wild type males. Paternal mitochondria numbers were assessed at different stages. **(A)** Paternal mitochondria numbers in 2 cell embryos were strikingly different in embryos from mothers treated with *ubc-18/ubc-16* and *ubc-18* RNAi. *lgg-1/lgg-2* RNAi knockdowns were used as a positive control for defective elimination of paternal mitochondria. **(B)** Quantification of paternal mitochondrial numbers in RNAi and mutant embryos. (n= 20 embryos). Data shown in graph are mean ± s.e.m. Differences between *fndc-1* and N2 via a student t-test had

the following p values: 1 cell 0.817, 2 cell 0.177, 4 cell 0.002, 8 cell 0.001. **(C)** *fndc-1* mutant CMXROS soaked males were mated with wild type hermaphrodites. A delay in removal of paternal mitochondria was observed until the 8-12 cell stage. Scale bar 10 μm.

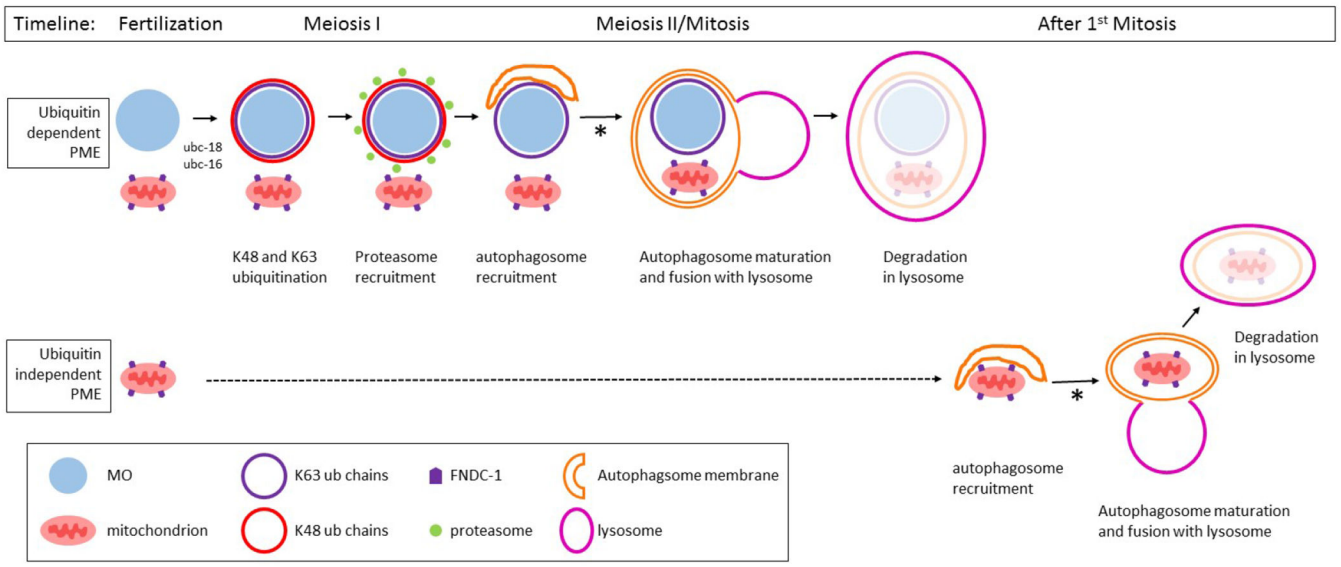

Figure 7. Model for the role of ubiquitination in the elimination of paternal mitochondria in *C. elegans*.

The targeting of paternal mitochondria for elimination (PME) after fertilization involves at least two separate pathways: ubiquitin dependent and ubiquitin independent pathways. In the ubiquitin dependent pathway, the membraneous organelles (MO) are quickly decorated with K48 (red) and K63 (blue) polyubiquitin chains. The MOs (light blue) and paternal mitochondria (pink) remain clustered together until the beginning of mitosis. The K48 chains recruit proteasomes (green) to the MO surface. K48 chains and proteasomes remain associated with the MOs for only a few minutes until the completion of meiosis I. After meiosis I, the autophagosome membranes (orange) are recruited to MOs and mitochondria. These autophagosomes presumably fuse with lysosomes and lead to the degradation of the enveloped MOs and mitochondria. Paternal mitochondria that escape the process described above can be degraded by a ubiquitin independent mechanism. The FNDC-1 protein (purple pentagon) localizes to the surface of paternal mitochondria, recruiting autophagosomal membranes via its LIR domain. These autophagsomes presumably fuse with lysosomes and lead to the degradation of the encased mitochondria. The process of autophagosomal maturation and lysosome fusion in both pathways requires the proteasomal associated ubiquitin recognition proteins RAD-23 and RPN-10 (denoted with an asterisk).

Table 1:

Strains used in this study

Strain Name	Genotype
LN130	*rcIs31* [*pie-1p*::GFP::Ub + *unc-119*(+)] II; *ltIs37[pie-1p::mCherry::his-58]*
LN153	*rcSi2[mex-5p::rpt-1::GFP + unc-119]II; ltIs37[pie-1p::mCherry::his-58]*
WY34	*ubc-18(ku354) III*
KWN775	*fndc-1(ry14) II; him-5(e1490) V*
VIG19	*mex-5p::GFP::lgg-1 II*
N2 (Bristol)	wild type